OPEN ACCESS Freely available online

ISSN: 0974-8369
Biology and Medicine

Research article

RBM10 Regulates LncRNA *SNHG17* Alternative Splicing to Suppress Colorectal Cancer Invasion Mechanism Research

Linxia An[1*], Peng Chen[1,2*], Yingshu Zhou[3], Miao He[4], Huifeng Li[4], Hongwei Zhao[3], Changhui Geng[3*]

[1]Department of Colorectal Surgery, Harbin Medical University Cancer Hospital, Harbin, People's Republic of China; [2]Department of Oncological Surgery, Chifeng Clinical Medical College, Inner Mongolia Medical University, Chifeng, People's Republic of China; [3]Department of General Surgery, The Fifth Affiliated Hospital of Harbin Medical University, Daqing, People's Republic of China; [4]Department of Pathology, Daqing Oilfield General Hospital, Daqing, People's Republic of China

ABSTRACT

Aim and Objective: To explore the role of *RBM10* in Colorectal Cancer (CRC) and the regulatory mechanism of CRC invasion through Alternative Splicing (AS) of long non-coding RNA (lncRNA) *SNHG17* by *RBM10*.

Methods: Samples were collected from sixty cases of CRC and their corresponding adjacent normal tissues. Immunohistochemistry and Western blot were performed to analyze the expression of *RBM10*. A Transwell invasion assay was conducted to evaluate the effect of *RBM10* on the invasion of HCT116 cells, and a Western blot was performed to detect the expression of EMT-related proteins. Moreover, CLIP-seq and RIP (RNA-Binding Protein Immunoprecipitation) experiments were performed to explore the interaction between *RBM10* and *SNHG17*.

Results: The expression of *RBM10* was significantly decreased in CRC tissues and cells compared to the normal adjacent tissues. Overexpression of *RBM10* inhibited CRC invasion, while knockdown of *RBM10* had the opposite effect. *RBM10* was found to interact with *SNHG17* and regulate its splice isoform balance. Specifically, the splice variant *SNHG17_2* regulated by *RBM10* was upregulated in CRC and was positively correlated with CRC invasion.

Conclusion: *RBM10* inhibits CRC invasion by regulating the alternative splicing of *SNHG17*, providing new research directions and potential targets for CRC treatment.

Keywords: *RBM10*; Colorectal cancer; *SNHG17*; Alternative splicing

INTRODUCTION

Colorectal Cancer (CRC) has emerged as the third most common malignant tumor globally, with approximately 1.9 million new cases and nearly 960,000 deaths annually [1]. In China, the incidence of CRC is increasing, with a trend towards younger patients [2].

Despite advances in treatment, the survival rate for advanced-stage patients remains below 50% due to the high invasiveness and metastasis rate of CRC [3]. Therefore, exploring the molecular mechanisms of invasion and metastasis in CRC holds great significance. In recent years, RNA Binding Proteins (RBPs) have gained attention in tumor research. Among them, *RBM10* was found to play an essential role in CRC, as it participates in the regulation of multiple signalling pathways and is closely related to metastatic CRC [4-7]. Alternative Splicing (AS) is a post-transcriptional gene expression regulation mechanism that plays a crucial role in various biological behaviors of tumors [8,9]. Our preliminary research revealed that *RBM10* has binding sites with long non-coding RNA *SNHG17*, suggesting that *RBM10* may affect the invasion and metastasis of CRC by regulating the AS of *SNHG17*. Based on these preliminary findings, this study aimed to explore the in-depth mechanism underlying the regulatory effects of *RBM10* on CRC invasion and metastasis through *SNHG17* AS. This research provides a better understanding of the mechanisms of tumor occurrence and new ideas for future therapeutic strategies.

Correspondence to: Linxia An, Department of Colorectal Surgery, Harbin Medical University Cancer Hospital, Harbin, People's Republic of China, E-mail: linxiaan@154.com

Peng Chen, Department of Colorectal Surgery, Harbin Medical University Cancer Hospital, Harbin, People's Republic of China, E-mail: chen@1352478.com

Changhui Geng, Department of General Surgery, The Fifth Affiliated Hospital of Harbin Medical University, Daqing, People's Republic of China, E-mail: gengchanghui@163.com

Received: 10-Jul-2024, Manuscript No. BLM-24-24655; **Editor assigned:** 12-Jul-2024, Pre QC No. BLM-24-24655 (PQ); **Reviewed:** 26-Jul-2024, QC No. BLM-24-24655; **Revised:** 02-Aug-2024, Manuscript No. BLM-24-24655 (R); **Published:** 09-Aug-2024, DOI: 10.35248/0974-8369.24.16.701.

Citation: An L, Chen P, Zhou Y, He M, Li H, Zhao H, et al. (2024) *RBM10* Regulates LncRNA *SNHG17* Alternative Splicing to Suppress Colorectal Cancer Invasion Mechanism Research. Bio Med. 16:701.

MATERIALS AND METHODS

Clinical samples

From October 2021 to October 2022, tumor samples were collected from surgical resections of 60 CRC patients from our hospital and collaborating units, along with their corresponding adjacent normal tissues. Among these samples, 37 were colon cancer cases and 23 were rectal cancer cases. Clear inclusion and exclusion criteria were established to ensure the quality and representativeness of the samples.

Inclusion criteria: CRC patients who visited our hospital or collaborating units within the specified date range.

Availability of surgically resected tumor samples and corresponding adjacent normal tissues (distance from tumor >3 cm). No chemotherapy or radiotherapy before surgery. Met the CRC diagnostic criteria defined by the World Health Organization. Patients or their families have provided written informed consent.

Exclusion criteria: Patients who have previously received or are currently receiving chemotherapy or radiotherapy. Patients with other concurrent malignant tumors or systemic diseases. Samples with insufficient quantity or poor quality those are unsuitable for subsequent experiments. Patients who did not provide written informed consent. This study followed the principles outlined in the Helsinki Declaration and was approved by our hospital's ethics committee. All tissue samples were immediately frozen in liquid nitrogen post-surgery and stored at -80°C for subsequent research. To ensure sample accuracy, all tissue samples were independently evaluated and confirmed by two experienced pathologists.

Cell culture

Human colon cancer cell line HCT116 cells (ATCC, CCL-247) were cultured in RPMI-1640 medium containing 10% Fetal Bovine Serum (FBS) and 1% penicillin-streptomycin. Human normal intestinal epithelial cell line HIEC-6 cells (ATCC, XY-XB2311) were cultured in DMEM medium containing 20% FBS and 1% penicillin-streptomycin. All cells were cultured at 37°C and 5% CO_2. When the cell density reached 80%-90%, passaging was performed in new culture flasks using 0.25% trypsin-EDTA solution for digestion followed by suspension in RPMI-1640 medium containing 10% FBS at a 1:3 ratio.

Cell transfection

Stable overexpression and knockdown of *RBM10* lentiviruses, as well as negative control vectors, were constructed by Shanghai GeneChem Co.Ltd. (Shanghai, China). HCT116 cells were cultured in six-well plates. When the cell density reached 70%-80%, they were passaged and then washed with Phosphate-Buffered Saline (PBS). Following the manufacturer's instructions, the lentiviruses and negative control virus were transfected into the cells. After 24 hours of lentiviral transfection, cells were selected in a puromycin-containing medium to establish stable overexpression and knockdown cell lines of the *RBM10* gene. Subsequently, *SNHG17* interference fragments were constructed by Suzhou GenePharma Co., Ltd. (Suzhou, China). HCT116 cells were cultured in six-well plates; when cell density reached 70%-80%, they were passaged and then washed with PBS. Plasmids were transfected into cell culture wells using a Lipofectamine 2000 reagent kit (Invitrogen) according to the manufacturer's instructions. Cells were cultured for 24 and 48 hours and then used for subsequent experiments.

Western blot

The cells were fully lysed in an immunoprecipitation assay buffer containing protease and phosphatase inhibitors (Beyotime, Jiangsu, China), and protein concentrations were determined using the BCA protein assay kit (Beyotime, Jiangsu, China). Protein samples (30 μg) were separated by 8%-15% SDS-PAGE gel electrophoresis and transferred to polyvinylidene difluoride membranes (PIVH00010, Merck Millipore, Burlington, MA, USA). After blocking for 2 hours, membranes were incubated overnight at 4°C with specific primary antibodies (diluted in PBS containing Tween-20), followed by 1.5 hours of incubation at room temperature with the corresponding secondary antibodies. The ECL detection kit (Merck Millipore, Burlington, MA, USA) was used for protein blotting, and Image J software (http://rsb.info.nih.gov/ij/, Bethesda, MD, USA) was employed for quantification. The primary antibodies included anti-*RBM10* (14423-1-AP, 1:500), GAPDH (60004-1-Ig, 1:5000) from Proteintech Group (Wuhan, China), and anti-N-cadherin (ab76011, 1:1000), anti-Vimentin (ab92547, 1:1000), and anti-E-cadherin (ab40772, 1:1000) from Abcam (Cambridge, MA, USA).

Reverse Transcription-quantitative Polymerase Chain Reaction (RT-qPCR)

Total RNA was extracted from tissues and cells using TRIzol reagent (Invitrogen, Carlsbad, CA, USA), and cDNA was obtained by reverse transcription using a kit (RR047A, Takara, Japan). RT-qPCR was performed using the SYBR Premix Ex TaqTM II (Perfect Real Time) kit (DRR081, Takara, Japan) on an ABI QuantStudio5 real-time PCR instrument (ABI, Foster City, CA, USA). Primers were synthesized by Shanghai Biotechnology Co., Ltd. (Shanghai, China), as shown in Table 1. Ct values for each well were recorded using β-actinas as an internal reference. The relative expression was calculated using the $2^{-\Delta\Delta Ct}$ method.

Table 1: RT-qPCR primer sequences.

Gene	Primer direction	Primer sequence
RBM10	Upstream	CCCGCAGTCTCAACAAACAA
	Down stream	TCATCTCGCAGGGAGCTGATA
SNHG17	Upstream	CCGTGAATCTCTTGGTGGTGTT
	Down stream	TGGTAGCCTCACTCTCCATTCTC
SNHG17_2	Upstream	CTGAGACCGTAGACCACTGTTAACAC
	Down stream	TGGTCAAACCCGTTCTGGAA
β-actin	Upstream	TACGCCAACACAGTGCTGTCT
	Down stream	TCTGCATCCTGTCGGCAAT

Immunohistochemistry

CRC tumor samples and adjacent paraffin-embedded specimens were sectioned into 4 μm slices using a slicer. The sections were stained using the Bond-Max automated immunohistochemistry staining system (Leica, Wetzlar, Germany). Thereafter, Image J software (http://rsb.info.nih.gov/ij/, Bethesda, MD, USA) was used for quantitative analysis of randomly captured 40x field images.

Transwell invasion assay

Matrigel (356234, Corning, Corning, NY, USA) was diluted with serum-free medium (1:8) and added to the upper chamber of transwell inserts. The inserts were placed in a 24-well plate and incubated at 37°C with 5% CO_2 for 2 hours. Cell density was adjusted to 105

cells/100 µL, with 100 µL added to the upper chamber and 500 µL of medium containing 15% serum added to the lower chamber, followed by incubation for 24 hours. The inserts were removed, and the Matrigel and cells in the upper chamber were wiped off with a cotton swab. The cells were fixed with 4% formaldehyde for 10 minutes, and stained with 0.1% crystal violet for 10 minutes. Invasion cells were counted using Image J software under a high-power microscope.

CLIP-Seq method

CLIP-Seq can reveal RNA-RBP interactions at the whole-genome level. CLIP-Seq technology involves coupling processed cell or tissue samples under 254 nm UV irradiation, capturing RNA through specific antibodies against RBPs, and forming protein-RNA complexes. Within the complex, RNA fragments protected by protein molecules are retained, while the remaining fragments are degraded to protect the target fragments. The ends of RNA fragments are labeled with radioactive phosphates, allowing separation of protein and RNA fragment complexes by denaturing SDS-PAGE gel, followed by autoradiography. Proteinase K degrades the protein components of protein-RNA complexes, preserving RNA components. RNA fragments are extracted and subjected to high-throughput sequencing. The CLIP-seq experiment was jointly completed by our research group and Appreciate the Beauty of Life, Inc (Wuhan, China).

RIP method

During the study, logarithmic growth phase HCT116 cells were collected and incubated for 1 hour at 4°C for dispersion. The cells were further incubated with magnetic beads and antibody mixtures for 2 hours to purify the final product. Following the instructions of Guangzhou Gene Seed Biotechnology Co.Ltd, RNA binding protein Immunoprecipitation (RIP) experiments were conducted using the RIP kit (product number: P0101). The antibodies used in this experiment include anti-*RBM10* antibodies (14,423-1-AP, Proteintech, Wuhan, China, dilution ratio: 1:500) and Goat Anti-Rabbit IgG (ab205718, Abcam, Cambridge, MA, USA, dilution ratio: 1:50).

Statistical methods

In this study, all data were collected from at least 3 independent experiments and presented in the form of mean ± standard deviation. All statistical analyses were performed using Microsoft Excel (Microsoft Corporation, USA) and GraphPad Prism v6.01 software (GraphPad Software, Inc, USA). Differences between two groups were evaluated by unpaired Student's *t*-test. Comparisons among multiple groups were analyzed with a one-way Analysis of Variance (ANOVA). In this study, a P value less than 0.05 was considered statistically significant.

RESULTS

Significantly decreased expression level of *RBM10* in CRC tissues

In this study, tissue samples were collected from 60 CRC patients, including 37 cases of colon cancer and 23 cases of rectal cancer. Moreover, corresponding adjacent normal tissue samples were collected. Immunohistochemistry and Western blot techniques were adopted to evaluate the expression level of *RBM10* protein in CRC tissues. The results showed that the expression level of *RBM10* in CRC tissues was significantly lower compared to adjacent normal tissues ($p<0.0001$; Figures 1A and 1B). In cellular experiments, the common CRC cell line HCT116 and the normal colon cell line HIEC-6 were selected for comparison. The results indicated that the expression level of *RBM10* in HCT116 cells was significantly lower than in HIEC-6 cells ($t=7.534$, $p<0.0001$; Figure 1C).

Overexpression of *RBM10* inhibits invasion and migration of HCT116 cells

To further investigate the functional role of *RBM10* in CRC invasion and metastasis, a series of *in vitro* functional experiments were conducted. Using lentiviral transduction technology, *RBM10* was successfully overexpressed and knocked down in HCT116 cells, and the transfection efficiency was validated by Western blot (Figure 2A). The Transwell invasion assay results revealed that overexpression of *RBM10* significantly inhibited the invasion and migration ability of cells compared to the control group ($t=5.97$, $p=0.004$). In contrast, the knockdown of *RBM10* significantly increased the invasion and migration ability of cells ($t=12.46$, $p<0.0002$) (Figure 2B). During the EMT process, overexpression of *RBM10* led to a significant decrease in N-cadherin ($t=3.68$, $p=0.004$) and Vimentin protein expression ($t=3.45$, $p=0.005$), while E-cadherin protein expression increased ($t=4.72$, $p=0.003$). Knockdown of *RBM10* produced the opposite effect, with a significant increase in N-cadherin ($t=4.78$, $p=0.001$) and Vimentin protein ($t=4.56$, $p=0.002$) expression, and a decrease in E-cadherin protein expression ($t=5.01$, $p<0.001$) (Figure 2C). Overall, our data suggest that *RBM10* plays an essential regulatory role in the invasion and metastasis of CRC cells, providing strong evidence for *RBM10* as a potential therapeutic target for CRC.

RBM10 regulates the alternative splicing of *SNHG17*

CLIP-seq analysis revealed the binding relationship between *RBM10* and 353 lncRNAs, among which the highest part in 10 peaks, *RBM10* has 3 significant binding sites with *SNHG17* (Table 2) (Figure 3). RIP experiments further confirmed the binding between *RBM10* and *SNHG17* and *SNHG17_2* (Figures 3A-3D). Interestingly, the overexpression of *RBM10* was negatively correlated with the expression level of *SNHG17*, as evidenced by the decreased expression level of *SNHG17* after *RBM10* overexpression ($t=3.89$, $p=0.004$); in contrast, after *RBM10* knockdown, the expression level of *SNHG17* demonstrated a significant increase ($t=4.12$, $p=0.003$) (Figure 3B).

Due to the lack of specific primers for *SNHG17_1*, its expression was inferred based on the expression changes of *SNHG17* and *SNHG17_2* and the proportion of *SNHG17_2* in *SNHG17*. *RBM10* overexpression was found to inhibit the expression of *SNHG17_2*, leading to a significant decrease in the proportion of *SNHG17_2* in *SNHG17*. However, *RBM10* knockdown promoted the expression of *SNHG17_2*, resulting in a significant increase in the proportion of *SNHG17_2* in *SNHG17* (Figures 3E and 3F). The results indicated that *RBM10* overexpression induced an increased expression of *SNHG17_1* ($t=3.45$, $p=0.007$); conversely, after *RBM10* knockdown, the expression of *SNHG17_1* significantly decreased ($t=3.12$, $p=0.009$) (Figure 3G). Collectively, these data revealed that *RBM10* balances the two splicing variants of *SNHG17 via* alternative splicing mechanisms.

SNHG17_2 is significantly upregulated in colorectal cancer cells/tissues and shows a negative correlation with *RBM10*

Real-time quantitative PCR detection revealed that *SNHG17_2* is significantly upregulated in the CRC cell line HCT116, while its expression is significantly decreased in normal colonic epithelial cells HIEC-6 ($t=18.03$, $p<0.0001$, (Figure 4A)). Furthermore, compared to adjacent normal tissues, *SNHG17_2* was significantly upregulated in CRC tissues ($t=4.214$, $p=0.0135$, (Figure 4B). Pearson correlation analysis was conducted and revealed a significant negative correlation between *RBM10* and *SNHG17_2* in CRC tissues ($R=-0.4549$, $p<0.05$) (Figure 4C). These research findings suggest a negative regulatory relationship between *RBM10* and *SNHG17_2* during the pathogenesis of CRC.

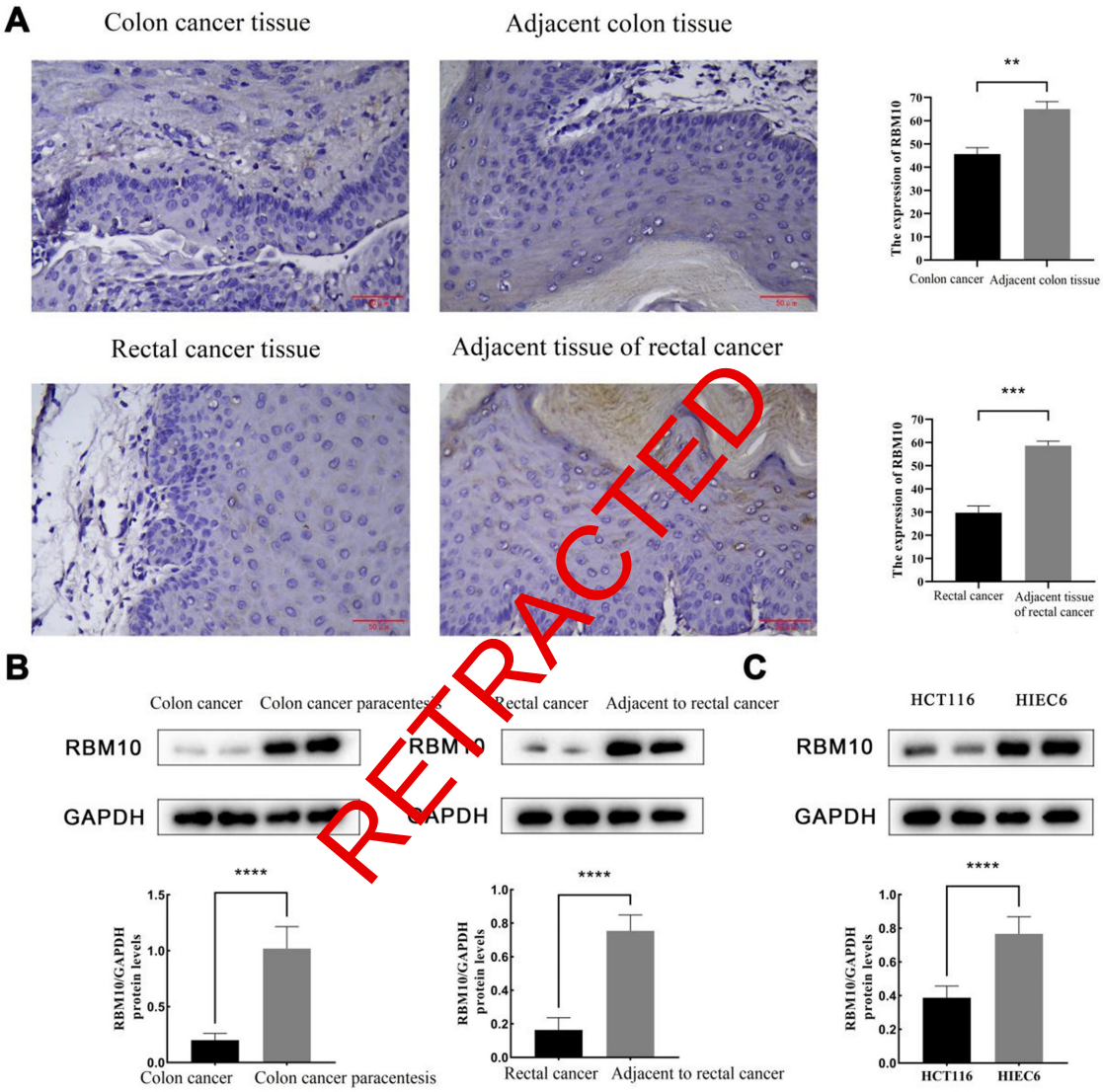

Figure 1: Expression Levels of *RBM10* in CRC Tissues and Cells, 1A: Immunohistochemical staining detecting the expression of *RBM10* protein in CRC tissues and corresponding adjacent normal tissues. (Scale bar: 50 μm), 1B: Western blot experiment detecting the expression level of *RBM10* protein in CRC tissues and corresponding adjacent normal tissues, 1C: Western blot experiment detecting the expression level of *RBM10* protein in HCT116 cells and HIEC-6 cells. **Note:** (**p<0.01, ***p<0.001, ****p<0.001).

Table 2: CLIP-seq analysis results.

lncRNA	Binding site range	Max height
MALAT1	65500207-65500506	47
NEAT1	65426044-65426131	46
NEAT1	65427561-65427687	45
CCAT1	127218383-127218652	43
SNHG17	38411123-38413456	43
SNHG17	38420567-38422901	39
NEAT1	65428653-65428731	37
NEAT1	65434190-65434501	35
CASC19	127185747-127185893	33
SNHG17	38431923-38433908	32

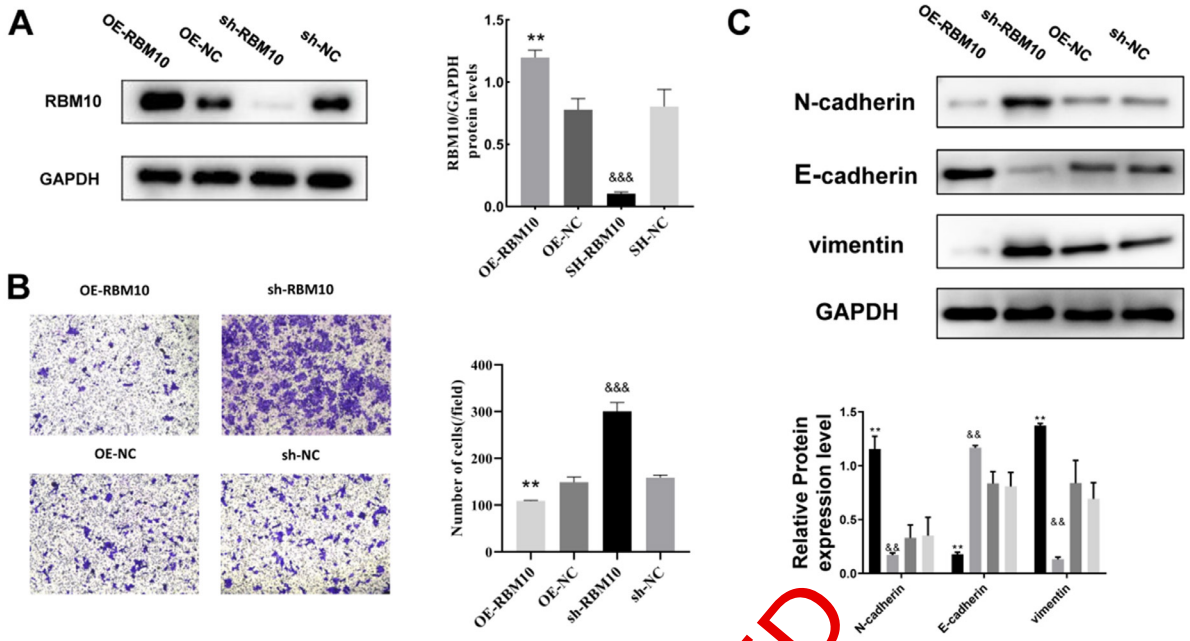

Figure 2: Study on the Regulation of CRC Cell Invasion and Migration by *RBM10*, 2A: Western blot experiment validating the overexpression and knockdown of *RBM10* in HCT116 cells, 2B: Transwell invasion assay demonstrating the effect of overexpression and knockdown of *RBM10* on cell invasion ability. 2C: Western blot experiment detecting the effect of overexpression and knockdown of *RBM10* on the expression of N-cadherin, Vimentin, and E-cadherin proteins. **Note:** (**p<0.01, compared to the OE-NC group; &&p<0.01, &&&p<0.001, compared to sh-NC group), (■): sh-*RBM10*10, (■): CE-*RBM10*, (■): OE-Nc, (■): sh-NC.

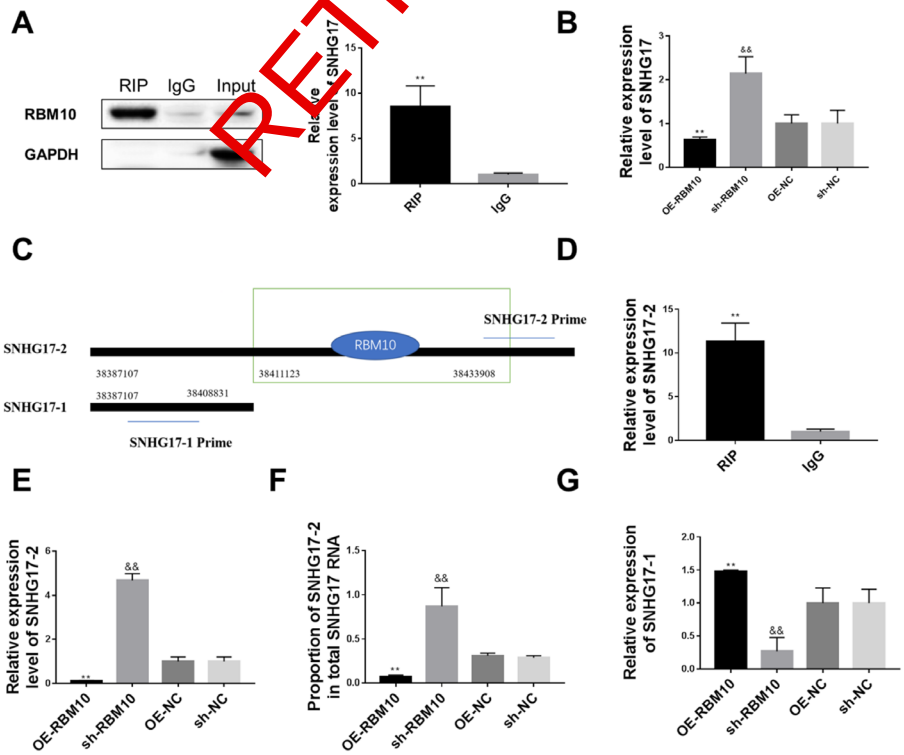

Figure 3: *RBM10* regulates the alternative splicing of *SNHG17*, 3A: RIP experiment detecting the binding between *RBM10* and *SNHG17*, 3B: RT-qPCR experiment evaluating the effects of *RBM10* overexpression and knockdown on the expression level of *SNHG17*, 3C: CLIP-seq analysis confirming that the main binding site of *RBM10* is located at 38411123-38433908 and concentrated on *SNHG17*_2, 3D: RIP experiment detecting the binding between *RBM10* and *SNHG17*_2, 3E: RT-qPCR experiment assessing the effects of *RBM10* overexpression and knockdown on the expression level of *SNHG17*_2, 3F: The proportion of *SNHG17*_2 in *SNHG17* after *RBM10* overexpression and knockdown, 3G: The effects of *RBM10* overexpression and knockdown on the expression level of *SNHG17*_1. **Note:** (**p<0.01, compared to OE-NC group for the OE-*RBM10* group; &&p<0.01, compared to sh-NC group for the sh-*RBM10* group).

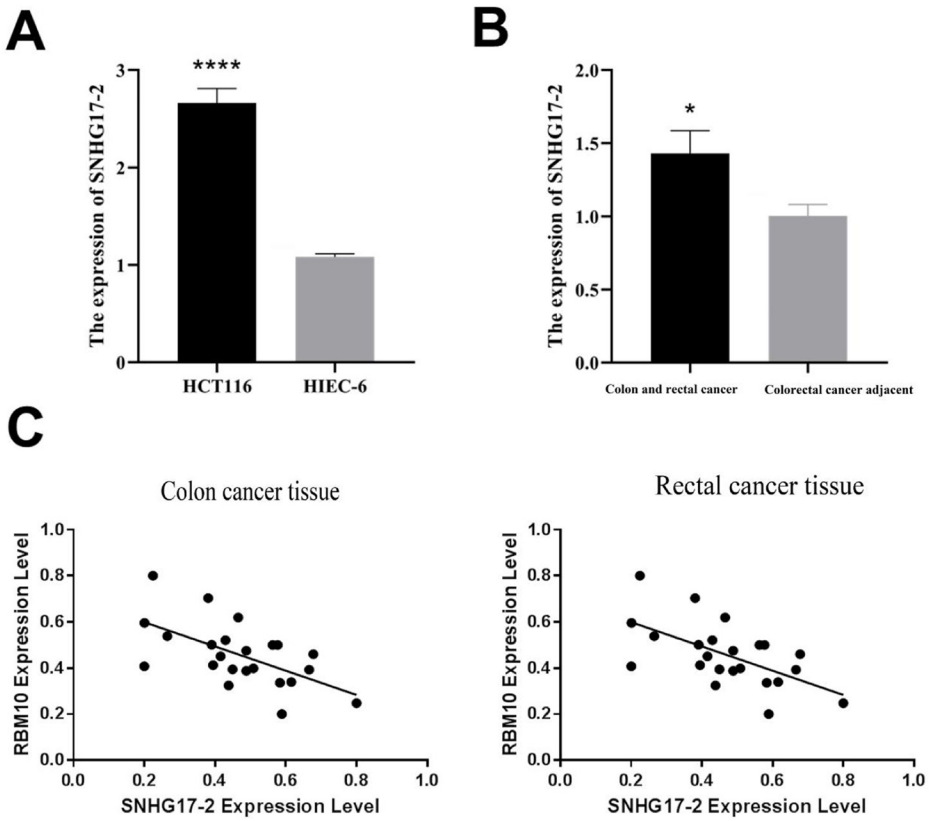

Figure 4: Downregulation of *SNHG17_2* expression in CRC cells and tissues and negative correlation with *RBM10*, 4A: RT-qPCR experiment detecting the expression of *SNHG17_2* in HCT116 cells and HIEC-6 cells. 4B: RT-qPCR experiment detecting the expression of *SNHG17_2* in CRC tissues and adjacent normal tissues, 4C: Pearson correlation analysis of the expression levels of *RBM10* and *SNHG17_2* in CRC tissues. **Note:** (*p<0.05, ****p<0.001)

RBM10 inhibits the invasion and migration of colon cancer HCT116 cells by suppressing *SNHG17_2*

In our study, *RBM10* knockdown HCT116 cells were selected as the research subject, and stable silencing of *SNHG17_2* was successfully achieved, revealing its functional role in this context (Figure 5A, t=4.23, p=0.002). Further invasion assays suggested that the invasion ability of cells after *SNHG17_2* silencing was significantly reduced compared to the control group (t=3.89, p=0.004, Figure 5B). In addition, detection of the expression of Epithelial-Mesenchymal Transition (EMT)-related proteins showed a decreased expression of N-cadherin (t=3.67, p=0.006) and Vimentin proteins (t=3.45, p=0.007) decreased after *SNHG17_2* silencing, while the expression of E-cadherin protein increased (t=3.12, p=0.009) compared to the control group (Figure 5C). These findings indicate the inhibitory role of *RBM10* against the invasion and migration of colon cancer HCT116 cells by suppressing *SNHG17_2*.

Expression levels of *RBM10* and *SNHG17_2* and analysis of clinical pathological data

This study explored the relationship between the expression of *RBM10* and *SNHG17_2* and the clinical pathological features of CRC patients in detail (Table 3). Firstly, among patients over 60 years old, *RBM10* was upregulated in 19 cases and downregulated in 11 cases (p=0.0707), while *SNHG17_2* was upregulated in 15 cases and downregulated in 20 cases. Regarding gender distribution, no significant difference was observed between high and low expressions of *RBM10* and *SNHG17_2* in both males and females. Regarding tumor location, for patients with right colon cancer, 12 cases demonstrated high expression of *RBM10* and 8 cases low expression, while 10 cases showed high expression of *SNHG17_2*, and another 10 cases low expression. Among rectal cancer patients, *RBM10* showed high expression in 15 cases and low expression in 8 cases, whereas 8 cases demonstrated high expression of *SNHG17_2* and 15 cases low expression. In terms of tumor size, patients with tumors smaller than 5 cm were associated with a significantly higher rate of *RBM10* overexpression compared to low expression (25 cases *vs.* 5 cases, p=0.00000093); in contrast, low *SNHG17_2* expressions was significantly more common than high expression (20 cases *vs.* 10 cases, p=0.0201). For patients with tumors larger than or equal to 5 cm, both high expression of *RBM10* and *SNHG17_2* were less common than low expression. In terms of tumor invasion depth, in stage T1, 20 cases demonstrated a high expression of *RBM10*, which was significantly more than the 10 cases with low expression (p=0.0242); however, high expression of *SNHG17_2* was observed in 6 cases, with 5 cases of low expression. Among patients in stage T3, 18 cases presented with high expression of *SNHG17_2*, which was significantly higher than the 8 cases with low expression. In terms of lymph node metastasis, both high expression of *RBM10* and *SNHG17_2* were found in 20 cases without lymph node metastasis, while only 10 cases were detected in patients with lymph node metastasis (p-value of 0.0201 for both), showing a significant correlation with lymph node metastasis. Lastly, in terms of the AJCC stage, 20 cases showed high expression of *RBM10* in stage I patients, which was significantly more than the 10 cases of low expression (p=0.0242). Both high and low expression of *SNHG17_2* included 5 cases, with a P value of 0.00894. Overall, these results revealed the potentially important roles of *RBM10* and *SNHG17_2* in the progression of CRC, especially in terms of tumor size, invasion depth, and lymph node metastasis.

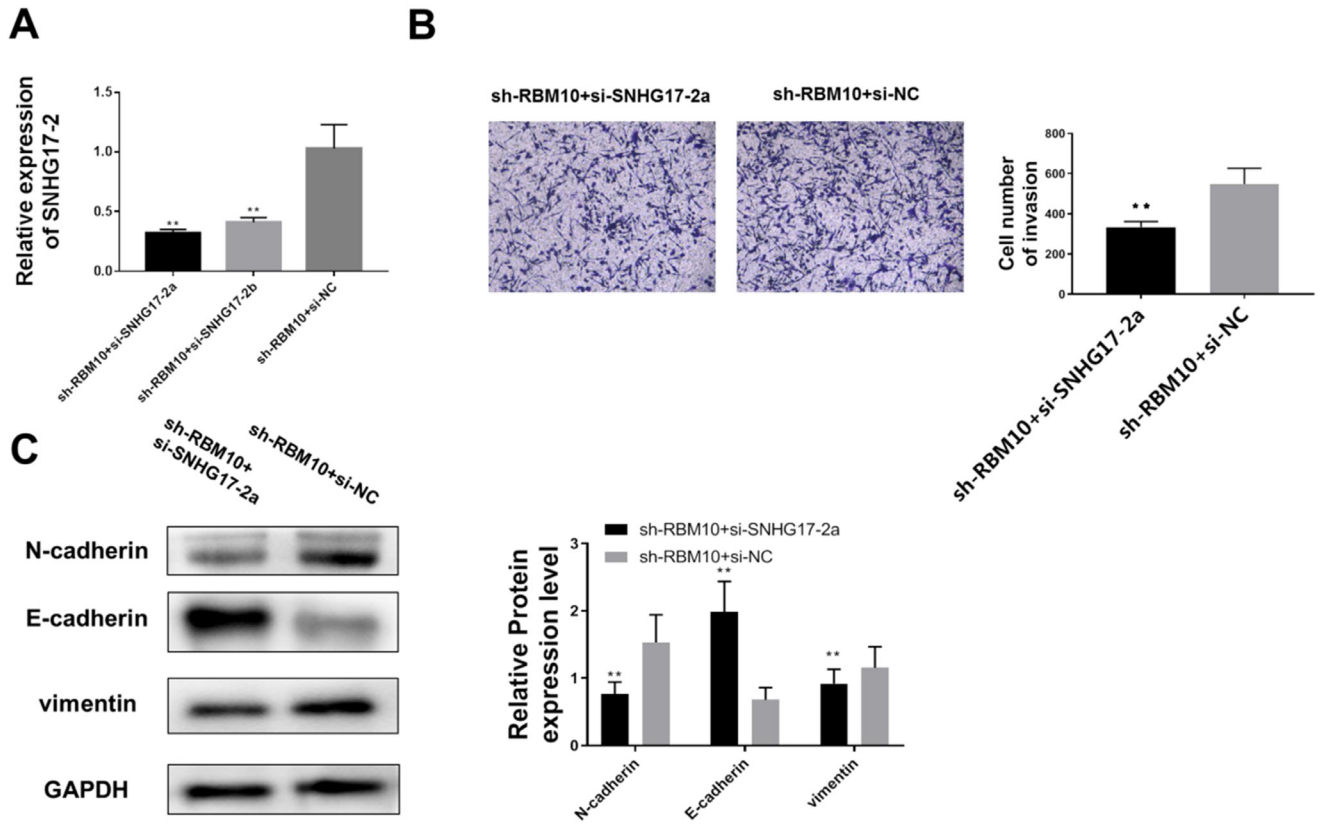

Figure 5: *RBM10* regulates *SNHG17_2* to inhibit the invasion and migration of colon cancer HCT116 cells, 5A: Western blot experiments verifying the silencing effect of *SNHG17_2* in *RBM10* knockdown HCT116 cells, 5B: Transwell invasion assays determining the effect of *SNHG17_2* silencing on cell invasion ability, 5C: Western blot experiments detecting the effect of *SNHG17_2* silencing on the expression of EMT-related proteins N-cadherin, Vimentin, and E-cadherin. **Note:** (**p<0.01).

Table 3: Expression levels and clinical pathological data analysis of *RBM10* and *SNHG17_2*.

Clinical pathological characteristics	*RBM10* high expression	*RBM10* low expression	p-value	*SNHG17_2* high expression	p-value
(years)					
>60	19	11	0.0707	15	0.2949
≤ 60	11	19		15	
Gender					
Female	16	14	0.7963	15	1
Male	14	16		15	
Tumor location					
Right colon	12	8	0.7506	10	1
Left colon	10	10		10	
Rectum	15	8		8	
Tumor size					
<5cm	25	5	0.00000093	10	0.0201
≥ 5cm	5	25		20	

Tumor invasion depth					
T1	20	10	0.0242	5	0.0252
T2	6	14		10	
T3	3	5		8	
T4	1	1		7	
Lymph node metastasis					
Absent	20	10	0.0201	10	0.0201
Present	10	20		20	
AJCC stage					
1st stage	20	10	0.0242	5	0.00894
2nd Stage	6	14		20	
3rd Stage	3	5		3	

DISCUSSION

RBM10 is a splicing factor closely related to the occurrence and development of various malignant tumors. However, its specific mechanism in CRC remains unclear. This study aimed to explore the function of *RBM10* in CRC and its potential mechanism and to investigate whether *RBM10* can inhibit the invasion of CRC by regulating the alternative splicing of *SNHG17*.

Currently, multiple studies have revealed frequent mutations of *RBM10* in CRC [9-11]. Bioinformatics studies further indicated that low *RBM10* expression was associated with reduced survival rates in CRC patients [12]. More importantly, single-gene cell mutations of *RBM10* in late-stage CRC patients were closely related to a brief progression-free survival period [13]. Consistently, a decrease in *RBM10* expression was observed in CRC tissues, while overexpression of *RBM10* significantly inhibited the invasion of CRC at the cellular level. During the invasion and metastasis of tumor cells, cells often lose epithelial characteristics and exhibit mesenchymal features, a process known as Epithelial-Mesenchymal Transition (EMT). EMT is also accompanied by an increase in N-cadherin and Vimentin and a decrease in E-cadherin [14-16]. Our findings demonstrate that *RBM10* can inhibit the expression of N-cadherin and Vimentin while promoting the expression of E-cadherin, further confirming the anticancer effect of *RBM10* in CRC. Clinical data analysis of CRC patients revealed that the expression of *RBM10* was significantly correlated with tumor size, depth of tumor invasion, presence of lymph node metastasis, and AJCC stage. Patients with low expression of *RBM10* often exhibit poorer pathological characteristics, consistent with our experimental findings, further confirming the important role of *RBM10* in the development, invasion, and metastasis of CRC.

As an RNA binding protein, *RBM10* plays a crucial role in alternative splicing, identifying and regulating multiple RNA motifs. Our experimental data demonstrate that *RBM10* can bind to 4040 types of RNA, including 353 types of lncRNA. Specifically, RIP experiments further confirmed the binding of *RBM10* to *SNHG17*.

Notably, *SNHG17* is considered an oncogene in CRC, and its abnormal expression is significantly associated with poor patient survival [16-18]. Liu et al., [19] reported that *SNHG17* promotes the proliferation, migration, and invasion of colon cancer cells and enhances their malignant characteristics through the miR-375/CBX3 axis. In addition, other studies have also shown that *SNHG17* is universally upregulated in various tissues and is significantly associated with tumor size, stage, and lymph node metastasis [20-22]. Our study further reveals that *RBM10* can regulate the alternative splicing of *SNHG17*, thereby influencing the behavior of CRC cells. Specifically, overexpression of *RBM10* reduces the expression of *SNHG17_2*, while silencing *RBM10* increases the expression of *SNHG17_2*.

CONCLUSION

The main contributions of this study are twofold. First, the findings confirm the role of *RBM10* in CRC as a tumor suppressor, which is mediated by regulating the alternative splicing of *SNHG17* to inhibit CRC invasion; second, the interaction between *RBM10* and *SNHG17* is clarified, providing a deeper understanding of the molecular mechanisms of CRC. Nevertheless, the limitations of the present study should be acknowledged. No *in vivo* experiments were carried out, and are required to further validate our findings; moreover, the detailed mechanism of action between *RBM10* and *SNHG17* remains incompletely understood. In the future, we plan to further study the role of *RBM10* and *SNHG17* in CRC in animal models to explore the interaction mechanism between the two.

CONFLICT OF INTEREST STATEMENT

The authors declares that there are no conflicts of interest.

FUNDING

Heilongjiang Provincial Health Commission Research Fund (20220404011047) Scientific Research Fund of Harbin Medical University Affiliated Fifth Hospital (2023-002).

AUTHOR CONTRIBUTIONS

*Co-first authors: All authors read and approved the final manuscript.

DATA AVAILABILITY STATEMENT

Data supporting this study are available in the Supplementary Information to the paper.

Electronic supplementary information

Supplemented with experimental results and data from Western blot of the four groups that support the results of this experiment.

REFERENCES

1. Siegel RL, Wagle NS, Cercek A, Smith RA, Jemal A. Colorectal cancer statistics, 2023. CA: A Cancer J. 2023;73(3):233-254.
2. Sedlak JC, Yilmaz OH, Roper J. Metabolism and colorectal cancer. Annu Rev Pathol. 2023;18(1):467-492.
3. Cervantes A, Adam R, Roselló S, Arnold D, Normanno N, Taïeb J, et al. Metastatic colorectal cancer: ESMO Clinical Practice Guideline for diagnosis, treatment and follow-up. Ann Oncol. 2023;34(1):10-32.
4. Rigaud VO, Hoy RC, Kurian J, Zarka C, Behanan M, Brosious I, et al. RNA-binding protein LIN28a regulates new myocyte formation in the heart through long noncoding RNA-H19. Circulation. 2023;147(4):324-337.
5. Jung JH, Lee H, Zeng SX, Lu H. *RBM10*, a new regulator of p53. Cells. 2020;9(9):2107.
6. Cao Y, Geng J, Wang X, Meng Q, Xu S, Lang Y, et al. RNA-binding motif protein 10 represses tumor progression through the Wnt/β-catenin pathway in lung adenocarcinoma. Int J Biol Sci. 2022;18(1):124.
7. Xu T, Zhang Y, Zhang J, Qi C, Liu D, Wang Z, et al. Germline profiling and molecular characterization of early onset metastatic colorectal cancer. Front oncol. 2020;10:568911.
8. Wan L, Yu W, Shen E, Sun W, Liu Y, Kong J, et al. SRSF6-regulated alternative splicing that promotes tumour progression offers a therapy target for colorectal cancer. Gut. 2019;68(1):118-129.
9. Wu L, Liu Q, Ruan X, Luan X, Zhong Y, Liu J, et al. Multiple Omics Analysis of the Role of *RBM10* Gene Instability in Immune Regulation and Drug Sensitivity in Patients with Lung Adenocarcinoma (LUAD). Bio Medicines. 2023;11(7):1861.
10. Liu Y, Liu X, Lin C, Jia X, Zhu H, Song J, et al. Noncoding RNAs regulate alternative splicing in Cancer. J Exp Clin Cancer Res. 2021;40(1):11.
11. Wang H, Yuan Z, Wang S, Pang W, Wang W, Liu X, et al. The comparison of risk factors for colorectal neoplasms at different anatomical sites. Int J Colorectal Dis. 2023;38(1):26.
12. Jung JH, Lee H, Zeng SX, Lu H. *RBM10*, a new regulator of p53. Cells. 2020;9(9):2107.
13. Guo L, Wang Y, Yang W, Wang C, Guo TA, Yang J, et al. Molecular profiling provides clinical insights into targeted and immunotherapies as well as colorectal cancer prognosis. Gastroenterol. 2023;165(2):414-428.
14. Tang Q, Chen J, Di Z, Yuan W, Zhou Z, Liu Z, et al. TM4SF1 promotes EMT and cancer stemness *via* the Wnt/β-catenin/SOX2 pathway in colorectal cancer. J Exp Clin Cancer Res. 2020;39:1-7.
15. Tan Z, Sun W, Li Y, Jiao X, Zhu M, Zhang J, et al. Current progress of EMT: A New Direction of targeted therapy for Colorectal Cancer with Invasion and Metastasis. Biomol. 2022;12(12):1723.
16. Bian Z, Zhou M, Cui K, Yang F, Cao Y, Sun S, et al. *SNHG17* promotes colorectal tumorigenesis and metastasis *via* regulating Trim23-PES1 axis and miR-339-5p-FOSL2-*SNHG17* positive feedback loop. J Exp Clin Cancer Res. 2021;40:1-4.
17. Office E. Erratum to long non-coding RNA *SNHG17* promotes gastric cancer progression by inhibiting P15 and P16. Transl Cancer Res. 2023;12(6):1647.
18. Ma L, Gao J, Zhang N, Wang J, Xu T, Lei T, et al. Long noncoding RNA *SNHG17*: A novel molecule in human cancers. Cancer Cell Int. 2022;22(1):104.
19. Zhang H, Wang SQ, Wang L, Lin H, Zhu JB, Chen R, et al. m6A methyltransferase METTL3-induced lncRNA *SNHG17* promotes lung adenocarcinoma gefitinib resistance by epigenetically repressing LATS2 expression. Cell Death Dis. 2022;13(7):657.
20. Pan X, Guo Z, Chen Y, Zheng S, Peng M, Yang Y, et al. STAT3-induced lncRNA *SNHG17* exerts oncogenic effects on ovarian cancer through regulating CDK6. Mol Ther Nucleic Acids. 2020;22:38-49.
21. Li X, Yuan Y, Pal M, Jiang X. Identification and validation of lncRNA-*SNHG17* in lung adenocarcinoma: A novel prognostic and diagnostic indicator. Front Oncol. 2022;12:929655.
22. Ma Z, Gu S, Song M, Yan C, Hui B, Ji H, Wang J, et al. Long non-coding RNA *SNHG17* is an unfavourable prognostic factor and promotes cell proliferation by epigenetically silencing P57 in colorectal cancer. Mol BioSyst. 2017;13(11):2350-2361.